Tissue distribution and subcellular localization of the family of Kidney Ankyrin Repeat Domain (KANK) proteins

Shiny Shengzhen Guo[1], Andrea Seiwert[1], Irene Y.Y. Szeto[1] and Reinhard Fässler[1]

[1]Department of Molecular Medicine, Max Planck Institute of Biochemistry, Martinsried, Germany

Running title: Tissue distributions of KANKs

Key words: KANK, expression, mouse, human, Western blot, immunostaining

Correspondence should be addressed to Shiny Shengzhen Guo (shguo@biochem.mpg.de)

Abstract

Kidney Ankyrin Repeat-containing Proteins (KANKs) comprise a family of four evolutionary conserved proteins (KANK1 to 4) that localize to the belt of mature focal adhesions (FAs) where they regulate integrin-mediated adhesion, actomyosin contractility, and link FAs to the cortical microtubule stabilization complex (CMSC). The human KANK proteins were first identified in kidney and have been associated with kidney cancer and nephrotic syndrome. Here, we report the distributions and subcellular localizations of the four *Kank* mRNAs and proteins in mouse tissues. We found that the KANK family members display distinct and rarely overlapping expression patterns. Whereas KANK1 is expressed at the basal side of epithelial cells of all tissues tested, KANK2 expression is mainly observed at the plasma membrane and/or cytoplasm of mesenchymal cells and KANK3 exclusively in vascular and lymphatic endothelial cells. KANK4 shows the least widespread expression pattern and when present, overlaps with KANK2 in contractile cells, such as smooth muscle cells and pericytes. Our findings show that KANKs are widely expressed in a cell type-specific manner, which suggests that they have cell- and tissue-specific functions.

Introduction

Kidney Ankyrin Repeat-containing protein (KANK1 or ANKRD15) was originally identified as a growth suppressor in human renal cell carcinoma (RCC) [1]. *In silico* analyses subsequently identified three additional KANK proteins (KANK2-4) in vertebrates [2] and one ortholog in *Drosophila melanogaster* (dKank) and *Caenorhabditis elegans* (VAB-19), respectively [3, 4]. The KANK proteins consist of a unique and conserved KANK-N-terminal (KN) motif, variable numbers of central coiled-coil domains and five C-terminal ankyrin repeats (ANKs) [3].

Genetic studies of the KANK family members have re-enforced the notion that they play prominent roles in kidney physiology and disease. Besides mutations in human *KANK1* promoting growth in RCC [1, 5, 6], recessive mutations in human *KANK1*, *KANK2* and *KANK4* were linked to nephrotic syndrome (NS)[7]. Furthermore, *KANK1* has been associated with neurodegenerative disease, such as cerebral palsy and spastic quadriplegic 2 (CPSQ2) [8]. Disruption of the *Kank2* gene in zebrafish leads to NS-like defects [7] and *in vivo* depletion of *dKank* in nephrocytes of *Drosophila melanogaster* results in the disruption of a highly specialized filtration structure that share notable similarities with the slit diaphragm of mammalian glomerular podocytes [7, 9]. In *Caenorhabditis elegans*, loss of the *Kank* orthologue *VAB-19* causes multiple abnormalities including epidermal detachment, defective axon outgrowth and the formation of gaps in basement membrane during vulva development [10-12]. Altogether, these observations point to a broad involvement of KANKs in development.

Studies with cultured cell lines revealed that KANK1-4 bind to and activate the integrin-binding and activating adaptor protein Talin, diminish actin stress fiber formation by inhibiting GEF-H1 release from microtubules (MTs), and curb integrin mechanotransduction by blocking actomyosin attachment to Talin [13-15]. Interestingly, fibroblasts and HeLa cells do not recruit KANK1-4 to nascent adhesions (NAs) but to the outer border or belt of focal adhesions (FAs) as well as to central fibrillar adhesions (FBs) [13, 15]. The FA belt-localized KANK proteins directly bind to Liprin-β and KIF21α and thereby link FAs to the cortical microtubule stabilization complex (CMSC), which regulates exocytosis of cargo such as MT1-MMP in the vicinity of FAs [13, 15-18]. It was also reported that KANK1 binds to the insulin receptor substrate (IRS) p53, which in turn

prevents association of IRSp53 with GTP-loaded Rac, activation of Arp2/3, and lamellipodia formation [19, 20]. The human KANK2 was also shown to regulate steroid receptor-mediated gene transcription by binding and sequestering steroid receptor coactivators in the cytoplasm [21]. Mutation that disrupts this function affects skin and hair morphogenesis, hinting at *KANK2* as a candidate gene for palmoplantar keratoderma and wooly hair in humans [22].

The pleotropic effects of KANK family members indicate intricate expression patterns. The aim of the present paper was to generate specific anti-KANK antibodies and to determine the expression patterns of KANK proteins in mouse tissues at the protein and mRNA levels. The specificity of the antibodies was controlled with tissue sections from KANK-null mice whose phenotypes will be reported elsewhere. The results of our experiments revealed that KANK1 is expressed in epithelial cells, while KANK2 is mainly found in mesenchymal cells. KANK3 is exclusively expressed in endothelial cells of blood and lymphatic vessels, and KANK4 only in few tissues, often co-expressed with KANK2.

Results

mRNA and protein expression of the KANK family in mouse tissues

The tissue distributions of the murine *Kank* mRNA expression was analyzed by qRT-PCR in indicated tissues of 8-week old mice (Fig. 1A). Primer pairs for each *Kank* gene flanking short introns were designed to ensure amplification of mRNA. The experiments revealed that *Kank1* is highly expressed in lung, skin and testis, slightly lower in adipose tissue, heart, kidney, ovary and stomach, and weakly in brain, liver and pancreas. *Kank2* was also expressed in most tissues examined, with the highest levels in lung, intermediate levels in adipose tissue, heart and testis, and lower levels in brain, kidney, liver, ovary, pancreas, skin and stomach. *Kank3* and *Kank4* displayed a restricted expression pattern with strong signals in lung, pancreas and testis.

To investigate protein expression, we synthesized peptides specific for each KANK protein, coupled them to a carrier protein and immunized rabbits. The specificity of the polyclonal antiserum was confirmed by Western blot experiments using a recently established mouse kidney fibroblast (MKF) cell line that exclusively expresses KANK2 [15]. As shown in Fig. 1B, the anti-KANK2 antibodies detected a protein of around 120 kDa in lysates of scrambled shRNA treated MKF cells, which was absent upon stable expression of a specific *Kank2* shRNA. To confirm the specificities of the other anti-KANK antibodies, a cDNA encoding the respective mouse *Kank* was expressed in *Kank2*-depleted MKF cells followed by Western blot analyses. The experiments revealed that our homemade antibodies recognized specific protein bands produced by each *Kank* cDNAs in the corresponding lysates with molecular weights of ~200 kDa for KANK1, ~100 kDa for KANK3, and ~150 kDa for KANK4.

Next, we determined the protein expression in lysates from different mouse tissues (Fig. 1C). In line with the qRT-PCR results, we found that all four KANK family members are highly expressed in lung. KANK2 protein is more widely expressed when compared to KANK1, 3 and 4. Interestingly, KANK1 and KANK3 are produced in at least two different molecular weights in pancreas, heart and muscle. Despite the high protein level in lung, KANK4 expression is low in most other tissues. Altogether these findings indicate that the four KANK family members are found in all tissues tested, albeit with variable levels. Since whole tissue lysates were analyzed in both qRT-PCR and

Western blot studies, we next perform immunofluorescence on representative tissues to pinpoint in which cell-types the KANK family members can be found.

Expression of KANK proteins in mouse kidney

In humans, *KANK1* mutations have been linked to RCC [1] and missense mutations in *KANK1*, *KANK2* and *KANK4* with nephrotic syndrome [7]. In line with a potential role in kidney, we found that KANK1-4 are expressed in kidney glomeruli (Fig. 2). KANK1 and KANK2 co-localize with Synaptopodin (SYNPO) in podocyte foot processes and are absent in $PECAM^+$ endothelial cells (Fig. 2A-2B, and Fig. S1B). KANK1 is additionally produced by the surrounding tubular epithelial cells where the protein is located at the plasma membrane (Fig. S1A). KANK2 and KANK4 are co-expressed throughout the cytoplasm of $PDGFR\beta^+$ mesangial cells and along the plasma membrane as well as in the cytoplasm of $PDGFR\beta^+$ pericytes surrounding the blood vessels, respectively (Fig. 2B1-B2, 2D, and Fig. S1C). Interestingly, KANK4 is absent in podocytes (data not shown), which express both KANK1 and KANK2 in their foot processes. KANK3 is expressed in $PECAM^+$ endothelial cells at the membrane and is absent in both podocytes and mesangial cells (Fig. 2C, and data not shown). The specificity of the signals was corroborated by staining tissue sections of kidneys from nullizygous mice (Fig. S2).

Altogether these expression data demonstrate that the KANK family members show distinct as well as partly overlapping expression patterns in kidney, indicating that mutations of the different *KANK* genes can indeed lead to kidney pathology.

Localization of KANKs in podocyte-like cells cultured *in vitro*

Since KANK1 and KANK2 are highly expressed in podocyte foot processes and are associated with nephrotic syndrome in humans, we decided to investigate the subcellular distributions of KANKs in mouse podocyte-like cells [23]. Laminin (LN) expression changes dynamically from LN111 to LN511 and finally to LN521 during glomerulogenesis in the glomerular basement membrane [24]. Podocytes are one of the major cell types secreting these LNs into the basement membrane. Interestingly, when the podocyte-like cells were seeded on LN511-coated surface, they assembled $Paxillin^+$ ring-shaped podosomes in the cell center and FAs in their periphery. KANK1 was readily detected in the podosome rings and weakly in peripheral FAs (Fig. 3A). However,

when the podocyte-like cells were seeded on LN111-coated surface, they fail to form podosomes, and instead only assemble FAs. Interestingly, podocytes seeded on LN111 distribute KANK1 in close vicinity of FAs, which likely represents CMSCs (Fig. 3C). Since LN521 was not available to us neither adhesion site formation nor KANK1 distribution on LN521 could be investigated.

KANK2, on the other hand, is weakly present in some podosomes of LN511-seeded cells (Fig. 3B) and accumulates, similarly like in fibroblasts seeded on FN [15], in the belt of peripheral FAs and in central adhesion of LN111-seeded podocytes (Fig. 3D). Consistent with the immunostaining of kidney sections (Fig. 2), neither KANK3 nor KANK4 are expressed in the podocyte-like cells. The specificities of the immunosignals were confirmed by blocking the antibodies with peptides used to generate the KANK antisera (data not shown).

KANK distributions in mouse lung and skin

In the lung we also observed expression of all KANK family members in a cell type-specific manner. KANK1 is expressed at the basal side of bronchial epithelial cells and is absent in type I (T1α^+) and type II (TTF1$^+$) alveolar epithelial cells (Fig. 4A), which express KANK2 at the plasma membrane (Fig. 4B and 4C; white arrowheads for T1α and yellow arrowheads for TTF1 positivity, respectively). KANK2 is also enriched at the plasma membrane of smooth muscle cells that line PECAM$^+$ endothelial cells of large and small vessels (Fig. 4D; arrow and asterisk). PECAM$^+$ endothelial cells only express KANK3, which is absent from all other cell types in lung (Fig. 4E, arrowheads). KANK4 is not expressed in epithelial cells but shares the expression with KANK2 at the plasma membrane of pericytes in capillaries (Fig. 4F).

In the epidermis of the mouse skin, KANK1 is enriched at the plasma membrane of basal and present throughout the cytoplasm of suprabasal keratinocytes (Fig. 5A; arrowhead and arrow). A similar expression pattern is observed in the hair follicles (Fig. 5A, asterisk). Epidermal and hair follicle keratinocytes lack expression of the other KANK family members (Fig. 5B and 5C, and data not shown). KANK2 is expressed along the plasma membrane of dermal fibroblasts (Fig. 5B1, arrowhead), pericytes surrounding the capillaries (Fig. 5B1, arrow), and Vimentin$^+$ cells surrounding the hair follicles (Fig. 5B2). KANK3 is exclusively expressed at the plasma membrane

of PECAM$^+$ endothelial cells of dermal vessels (Fig. 5C), and KANK4 expression is barely detectable in mouse skin (data not shown).

KANK expression in mouse brain

In the brain parenchyma of adult mice, we only observed expression of KANK1 in GFAP$^+$ astrocytes within the medulla oblongata (Fig. 6A), while no specific signals for KANK1 could be found in the cortex, midbrain and cerebellum. KANKs are absent in the foot process of astrocytes adjacent to the brain capillaries, whereas KANK2 is found in NG2$^+$ pericytes (Fig 6B) and KANK3 in PECAM$^+$ endothelial cells of these capillaries (Fig. 6C). KANK4 was not detected in the brain (data not shown).

KANK1 has been linked to cerebral palsy and spastic quadriplegic 2 (CPSQ2) where brain atrophy and ventriculomegaly had been observed by neuroimaging [8]. Ventriculomegaly can result from abnormal absorption and/or production of cerebrospinal fluid by the choroid plexus (ChP). Interestingly, in the brain harvested at embryonic day (ED) 14.5, KANK1 localizes to the basal side of ependymal cells (epithelial cells) of the ChP, while KANK2 and KANK3 are present in the stromal and endothelial cells of the ChP core, respectively (Fig.6D-F). KANK4 was not detected. In the telencephalic ChP of the adult brain, KANK1 is absent from ependymal cells, while KANK2 and KANK3 remain expressed in NG2$^+$ pericytes and PECAM$^+$ endothelial cells, respectively (data not shown).

Expression of KANKs in the mouse vasculature

Similarly like in kidney, lung, brain and all other organs analyzed so far, in the aorta, KANK2 is also strongly expressed throughout the cytoplasm of αSMA$^+$ muscle cells of the tunica media layer (Fig. 7A) and KANK3 in PECAM$^+$ endothelial cells (Fig. 7B). KANK1 as well as KANK4 are absent in cells of the aorta (data not shown).

In the mouse retina, KANK2 is expressed in the PDGFRβ^+ pericytes (Fig. 7C, arrows) but not in the endothelial cells (Fig. S3A, arrowheads). KANK3, in contrast, is present in PECAM$^+$ endothelial cells of the vascular tube as well as in sprouting tip cells (Fig. 7D, arrowheads indicating sprouting cells) and absent from PDGFRβ^+ pericytes (Fig. S3B, arrows).

Finally, we stained tissue sections of spleen to test whether KANK3 is expressed in lymphatic in addition to blood endothelial cells. KANK3 is found at the plasma membrane of VEGFR3$^+$ lymphatic endothelial cells (Fig. 7E).

KANK protein distributions in mouse esophagus

Since KANK4 is found in contractile mesangial cells (kidney) but absent from vascular NG2$^+$ pericytes (brain) and αSMA$^+$ muscle cells (aorta), we decided to investigate the distribution of KANK proteins in the esophagus which consist of a stratified layer of epithelial cells that is surrounded by a thick layer of smooth muscle cells. Cross-sections revealed that KANK1 is enriched at the basal side and in the cytoplasm of the stratified squamous epithelial cell layers (Fig 8A, arrowhead indicating the basal side). KANK1 is absent in αSMA$^+$ smooth muscle cells, which strongly express KANK2 in the cytoplasm and along the entire plasma membrane (Fig. 8B). KANK3 was found in PECAM$^+$ endothelial cells (Fig. 8C, arrowheads) and KANK4 was not expressed in the smooth muscle cells of the esophagus (Fig. 8D, asterisk indicating non-specific signals), indicating that KANK4 expression is restricted to a very limited population of contractile cells.

Discussion

The KANK protein family consists of 4 members and was initially linked to nephrotic syndrome and kidney cancer [1, 6]. In the present paper, we report the generation of specific, polyclonal peptide antisera against mouse KANK1, 2, 3 and 4, which we used to determine their expression pattern in mouse tissues. The antibodies produced KANK isoform-specific signals on Western blots, and moreover, revealed a cell type-specific expression pattern in PFA-fixed mouse tissue sections.

Our immunostaining demonstrated KANK1 expression in epithelial cells of all organs that were tested in this study. KANK1 localized to the basal side of basal keratinocytes, bronchial and esophageal epithelial cells, and around the entire plasma membrane and in the cytoplasm of suprabasal cells of the epidermis and esophagus. This staining pattern indicates that in some tissues KANK1 localizes to integrin adhesion sites at basal plasma membrane domains and in other tissues KANK1 expression extends to basolateral and apical plasma membrane domains. KANK2 was mainly found in mesenchymal cells including mesangial cells in kidney glomeruli (throughout the cytoplasm), pericytes, tissue fibroblasts (at the plasma membrane) and vascular smooth muscle cells (at the plasma membrane and in the cytoplasm). Notable exceptions were alveolar cells of the lung and podocytes of kidney glomeruli, in which KANK2 is strongly expressed along the plasma membrane. KANK3 is expressed in all tissues analyzed where it was exclusively found in endothelial cells of blood and lymphatic vessels. KANK4 expression is restricted to mesenchymal cells of few tissues including lung and kidney. In kidney, KANK4 co-localizes with KANK2 in the cytoplasm of mesangial cells and vascular pericytes. Mutations in KANK1, KANK2 and KANK4 were shown to cause nephrotic syndrome in humans [1]. Although our immunostaining supports this notion, the cell type-specific expression of the KANKs hints at specific functions that, when lost, may lead to distinct kidney pathologies.

Our experiments also revealed a substrate-dependent distribution of KANK1 and KANK2 in podocyte-like cells. This is of interest, as podocytes express and deposit different laminins in a highly dynamic manner during glomerulogenesis: the first LN deposited into glomerular basement membranes is LN111, which is then replaced by LN511, which in turn is finally substituted by LN521 [24]. Mouse podocyte cells (established by Nicolaou et al., 2012 [23])

seeded on LN111 assembled numerous peripheral and central FAs, which accumulated KANK2 along the FA belt [15] and KANK1 in CMSCs that are in close vicinity of FAs [13, 15]. Interestingly, podocyte cells cultured on LN511 assembled Paxillin-positive ring-shaped podosomes in the cell center and FAs in the cell periphery. KANK1 and KANK2 are expressed in the podosomal rings, and adjacent to the peripheral FAs. Unfortunately, adhesion site assembly as well as KANK1 and KANK2 distributions in podocytes seeded on LN521 could not be analyzed, as LN521 was not available to us. Nevertheless, our observations strongly indicate that mutations in *KANK1* and *KANK2*, although expressed in the same cell type, probably affect the kidney filtration unit differently and hence, may cause specific subtypes of nephrotic syndromes.

Interestingly, we found no KANKs expressed in neurons. A reason for the absence of KANKs in neurons may be due to the molecular composition of the MT attachment complex at plasma membranes of epithelial cells versus presynaptic membranes of neurons. At sites of exocytosis in epithelial cells, KANK1 is recruited to the CMSC through direct binding to Liprin-β1. In neurons, exocytosis of neurotransmitters occurs at the active zone (CAZ) of the presynaptic membrane. CAZs share components of CMSC such as ELKS and Liprin-α, however, neither LL5 nor the KANK-binding Liprin-β are found in CAZs [25, 26]. The absence of Liprin-β, which recruits KANK1 to the CMSC in epithelial cells, is probably the reason why KANK1 is not required to co-ordinate MT attachment and hence, not needed in neurons. Interestingly, we observed KANK1 expression in $GFAP^+$ astrocytes in the medulla oblongata, but not in astrocytes of other brain regions. The reason for this region-specific astrocyte expression of KANK1 is unclear. We also found that KANK proteins are expressed in the ChP: in embryonic ChP, KANK1 is expressed in ependymal cells developed from the neuroepithelium, KANK2 in stromal cells that are derived from the head mesenchyme and KANK3 in endothelial cells. KANK1 expression vanishes in the ChP of adult mice pointing to a specific role of KANK1 in ChP during fetal period.

In summary, KANK proteins show a cell type-specific expression pattern, which rarely overlaps, suggesting their potential specific function(s) during mammalian development, postnatal homeostasis and diseases. To address the *in vivo* function of the KANK proteins, we generated KANK1-4-null mouse strains that are currently analyzed for their loss-of-function phenotypes.

These studies will certainly shed light on the functional properties of this new and interesting family of adaptor proteins.

Materials and Methods

Tissue sampling

Wild-type (WT) C57BL/6N mice were obtained from the animal facility at the Max-Planck Institute of Biochemistry, Martinsried, Germany. Mice were bred in a special pathogen-free mouse facility and all animal experiments were conducted in accordance with the protocol approved by the government of Upper Bavaria.

Female KANK1-, KANK2-, KANK3-, KANK4-null and WT littermate mice were euthanized at 4 to 12 months of age to isolate desired organs. For immunostaining, tissues were fixed in 4% paraformaldehyde (PFA) for 4h at 4°C, equilibrated in 30% sucrose overnight at 4°C, embedded in Cryomatrix (Thermo Scientific, 6769006) and cryosectioned at 7-10 µm.

Cell culture

Stable depletion of *Kank2* in the SV40 large T-immortalized mouse kidney-derived fibroblasts (MKF) [15] and the generation of the mouse podocyte-like epithelial cells [23] have been previously described and were used to analyze the specificity of the homemade KANK antibodies and the subcellular localization of KANKs. MKFs were cultured in DMEM (Gibco, 31966-021) supplemented with 10% FBS, Penicillin/Streptomycin (Gibco, 15140-122) and MEM NEAA (Gibco, 11140-35). Mouse podocyte-like cells were cultured in Keratinocyte-SFM medium (Gibco, 10725-018).

Plasmids and transient transfection

The expression plasmid for each mouse *Kank* was subcloned from peGFP-N1-KANKs (Sun et al., 2016) into the pcDNA3.1(-) vector. *Kank1* was cloned with restriction sites *Xho*I and *Eco*RI, *Kank3* with *Xba*I and *Eco*RI, and *Kank4* with *Nhe*I and *Xho*I into the pcDNA3.1(-) vector. The plasmids were transfected using Lipofectamine™ 2000 Transfection Reagent according to the manufacturer's instructions (Invitrogen, 11668-019).

Quantitative real time-PCR (qRT-PCR)

Indicated mouse organs were isolated from 8-week old WT mice. Total RNA was extracted with RNeasy Mini extraction kit (Qiagen, 74104) and transcribed into cDNA with the iScript cDNA Synthesis Kit (Biorad, 170-8891). Real time PCR was performed with the LightCycler®480

Instrument II (Roche). PCR protocol: 5 min. 95°C; 40 x (15 sec 95°C, 15 sec 68°C (*Kank1*, *2*, *4*)/ 15 sec 65°C (*Kank3*)); 15 sec 95°C; 15 sec 60°C; 15 sec 95°C; ∞ 4 °C. Samples were measured in triplicates. *Kank* levels in different tissues were first normalized to *Gapdh* levels and then plotted relative to the expression level of the tissue with the lowest level, which was set to 1. In the *Kank1* and *Kank2* analyses, expression levels of spleen were set to 1, and in the *Kank3* and *Kank4* analyses, expression levels of liver were set to 1. PCR primers are listed in Tab. S1.

Antibody production and affinity purification

Specific and unique peptides were synthesized for each KANK protein. Sequences are listed in Tab. S2. The peptides carried either an N- or C-terminal cysteine residue for coupling with the carrier protein. TiterMax Gold Adjvant (Sigma, T2684) was used for the first and incomplete Freund's Adjuvant (Sigma, F5506) was used for the subsequent three immunizations of rabbits. Final serum was tested by Western blot and purified with the Melon^{TM} Gel IgG purification Kit (Thermofisher, 45212) following manufacturer's instructions.

Protein isolation and Western blot

Cells were washed once with PBS, lysed with RIPA buffer supplemented with protease inhibitors (Roche, 04693159001) and incubated for 20 min on ice followed by centrifugation for 20 min at maximum speed at 4°C.

Tissue organs from mice were snap-frozen in liquid nitrogen, homogenized using the Ultra-Turrax T8 disperser (IKA) and lysed with RIPA buffer and further processed as described above.

The cell and tissue lysates were then separated by 10% SDS gel, transferred onto pre-activated PVDF membranes (Immobilon-P, Merck KGaA, IPVH00010). After blocking with 3% BSA in PBST for 1 h at RT, membranes were incubated with the indicated primary antibodies overnight at 4°C. Anti-mouse or anti-rabbit-HRP secondary antibodies were applied for 1 h at RT and the membranes were developed with Chemiluminescent HRP substrate (Millipore, P90720). The antibody dilutions are listed in Tab. S3.

Immunofluorescence

Cryosections were washed with PBS three times and antigen retrieval was performed if necessary. The sections were permeabilized in 0.1% Triton X-100 for 15 min and blocked in PBS

supplemented with 3-5% BSA for 2h at RT. Sections were incubated with primary antibody overnight at 4°C, washed five times with PBS, incubated with secondary antibody for 2h at RT, washed five times with PBS and stained with DAPI for 10 min at RT. Finally, sections were mounted with Elvanol. Images were taken on a Zeiss (Jena) LSM780 confocal laser scanning microscope. The antibody dilutions are listed in Tab. S3.

WT podocyte-like cells were cultured on 4-well chamber slides (ibidi, 80427) coated with either 0.5 µg/cm^2 laminin iMatrix-511 (LN5111) (Matrixome, 892 012) or 2 µg/cm^2 mouse laminin LN111 (Invitrogen, 23017-015) for 1h at 37°C. The immunofluorescent staining was performed as described above. Staining for KANKs on these cells was controlled by blocking the primary KANK antibody with the peptides used to generate the antiserum (Tab. S2). Both, the KANK antibodies and the blocking peptides were incubated in a 1:30 ratio for 1h at RT before applying to the cells.

Whole mount staining of postnatal retinas

Eyes were isolated from WT mice at postnatal day 7 (P7), fixed in 4% PFA for 2h on ice. Retinas were dissected, flattened on drops of cold methanol, incubated in blocking solution (PBS supplemented with 0.3% Triton-X-100, 0.2% BSA, 5% goat serum) overnight at 4°C, incubated with primary antibodies overnight at 4°C, washed five times with PBS supplemented with 0.3% Triton-X-100 at RT, incubated with secondary antibodies at 4°C overnight, washed five times with PBS supplemented with 0.3% Triton-X-100 and mounted with Elvanol under the microscope.

Acknowledgements

We are grateful to the employees of our animal house. The work was supported by the ERC and Max Planck Society.

References

[1] S. Sarkar, B.C. Roy, N. Hatano, T. Aoyagi, K. Gohji, R. Kiyama, A novel ankyrin repeat-containing gene (Kank) located at 9p24 is a growth suppressor of renal cell carcinoma, J Biol Chem 277 (2002) 36585-36591.

[2] Y. Zhu, N. Kakinuma, Y. Wang, R. Kiyama, Kank proteins: a new family of ankyrin-repeat domain-containing proteins, Biochim Biophys Acta 1780 (2008) 128-133.

[3] N.P. Chen, Z. Sun, R. Fassler, The Kank family proteins in adhesion dynamics, Curr Opin Cell Biol 54 (2018) 130-136.

[4] M.R. Hensley, Z. Cui, R.F. Chua, S. Simpson, N.L. Shammas, J.Y. Yang, Y.F. Leung, G. Zhang, Evolutionary and developmental analysis reveals KANK genes were co-opted for vertebrate vascular development, Sci Rep 6 (2016) 27816.

[5] B.C. Roy, T. Aoyagi, S. Sarkar, K. Nomura, H. Kanda, K. Iwaya, M. Tachibana, R. Kiyama, Pathological characterization of Kank in renal cell carcinoma, Exp Mol Pathol 78 (2005) 41-48.

[6] N. Kakinuma, Y. Zhu, Y. Wang, B.C. Roy, R. Kiyama, Kank proteins: structure, functions and diseases, Cell Mol Life Sci 66 (2009) 2651-2659.

[7] H.Y. Gee, F. Zhang, S. Ashraf, S. Kohl, C.E. Sadowski, V. Vega-Warner, W. Zhou, S. Lovric, H. Fang, M. Nettleton, J.Y. Zhu, J. Hoefele, L.T. Weber, L. Podracka, A. Boor, H. Fehrenbach, J.W. Innis, J. Washburn, S. Levy, R.P. Lifton, E.A. Otto, Z. Han, F. Hildebrandt, KANK deficiency leads to podocyte dysfunction and nephrotic syndrome, J Clin Invest 125 (2015) 2375-2384.

[8] I. Lerer, M. Sagi, V. Meiner, T. Cohen, J. Zlotogora, D. Abeliovich, Deletion of the ANKRD15 gene at 9p24.3 causes parent-of-origin-dependent inheritance of familial cerebral palsy, Hum Mol Genet 14 (2005) 3911-3920.

[9] H. Weavers, S. Prieto-Sanchez, F. Grawe, A. Garcia-Lopez, R. Artero, M. Wilsch-Brauninger, M. Ruiz-Gomez, H. Skaer, B. Denholm, The insect nephrocyte is a podocyte-like cell with a filtration slit diaphragm, Nature 457 (2009) 322-326.

[10] M. Ding, A. Goncharov, Y. Jin, A.D. Chisholm, C. elegans ankyrin repeat protein VAB-19 is a component of epidermal attachment structures and is essential for epidermal morphogenesis, Development 130 (2003) 5791-5801.

[11] S. Ihara, E.J. Hagedorn, M.A. Morrissey, Q. Chi, F. Motegi, J.M. Kramer, D.R. Sherwood, Basement membrane sliding and targeted adhesion remodels tissue boundaries during uterine-vulval attachment in Caenorhabditis elegans, Nat Cell Biol 13 (2011) 641-651.

[12] Y. Yang, W.S. Lee, X. Tang, W.G. Wadsworth, Extracellular matrix regulates UNC-6 (netrin) axon guidance by controlling the direction of intracellular UNC-40 (DCC) outgrowth activity, PLoS One 9 (2014) e97258.

[13] B.P. Bouchet, R.E. Gough, Y.C. Ammon, D. van de Willige, H. Post, G. Jacquemet, A.M. Altelaar, A.J. Heck, B.T. Goult, A. Akhmanova, Talin-KANK1 interaction controls the recruitment of cortical microtubule stabilizing complexes to focal adhesions, Elife 5 (2016).

[14] N.B.M. Rafiq, Y. Nishimura, S.V. Plotnikov, V. Thiagarajan, Z. Zhang, S. Shi, M. Natarajan, V. Viasnoff, P. Kanchanawong, G.E. Jones, A.D. Bershadsky, A mechano-signalling network linking microtubules, myosin IIA filaments and integrin-based adhesions, Nat Mater 18 (2019) 638-649.

[15] Z. Sun, H.Y. Tseng, S. Tan, F. Senger, L. Kurzawa, D. Dedden, N. Mizuno, A.A. Wasik, M. Thery, A.R. Dunn, R. Fassler, Kank2 activates talin, reduces force transduction across integrins and induces central adhesion formation, Nat Cell Biol 18 (2016) 941-953.

[16] N. Kakinuma, R. Kiyama, A major mutation of KIF21A associated with congenital fibrosis of the extraocular muscles type 1 (CFEOM1) enhances translocation of Kank1 to the membrane, Biochem Biophys Res Commun 386 (2009) 639-644.

[17] S. Stehbens, T. Wittmann, Targeting and transport: how microtubules control focal adhesion dynamics, J Cell Biol 198 (2012) 481-489.
[18] B. van der Vaart, W.E. van Riel, H. Doodhi, J.T. Kevenaar, E.A. Katrukha, L. Gumy, B.P. Bouchet, I. Grigoriev, S.A. Spangler, K.L. Yu, P.S. Wulf, J. Wu, G. Lansbergen, E.Y. van Battum, R.J. Pasterkamp, Y. Mimori-Kiyosue, J. Demmers, N. Olieric, I.V. Maly, C.C. Hoogenraad, A. Akhmanova, CFEOM1-associated kinesin KIF21A is a cortical microtubule growth inhibitor, Dev Cell 27 (2013) 145-160.
[19] N. Kakinuma, B.C. Roy, Y. Zhu, Y. Wang, R. Kiyama, Kank regulates RhoA-dependent formation of actin stress fibers and cell migration via 14-3-3 in PI3K-Akt signaling, J Cell Biol 181 (2008) 537-549.
[20] B.C. Roy, N. Kakinuma, R. Kiyama, Kank attenuates actin remodeling by preventing interaction between IRSp53 and Rac1, J Cell Biol 184 (2009) 253-267.
[21] Y. Zhang, H. Zhang, J. Liang, W. Yu, Y. Shang, SIP, a novel ankyrin repeat containing protein, sequesters steroid receptor coactivators in the cytoplasm, EMBO J 26 (2007) 2645-2657.
[22] Y. Ramot, V. Molho-Pessach, T. Meir, R. Alper-Pinus, I. Siam, S. Tams, S. Babay, A. Zlotogorski, Mutation in KANK2, encoding a sequestering protein for steroid receptor coactivators, causes keratoderma and woolly hair, J Med Genet 51 (2014) 388-394.
[23] N. Nicolaou, C. Margadant, S.H. Kevelam, M.R. Lilien, M.J. Oosterveld, M. Kreft, A.M. van Eerde, R. Pfundt, P.A. Terhal, B. van der Zwaag, P.G. Nikkels, N. Sachs, R. Goldschmeding, N.V. Knoers, K.Y. Renkema, A. Sonnenberg, Gain of glycosylation in integrin alpha3 causes lung disease and nephrotic syndrome, J Clin Invest 122 (2012) 4375-4387.
[24] J.H. Miner, Developmental biology of glomerular basement membrane components, Curr Opin Nephrol Hypertens 7 (1998) 13-19.
[25] R.G. Held, P.S. Kaeser, ELKS active zone proteins as multitasking scaffolds for secretion, Open Biol 8 (2018).
[26] I. Noordstra, A. Akhmanova, Linking cortical microtubule attachment and exocytosis, F1000Res 6 (2017) 469.

Figure legends

Fig. 1. Tissue distributions of *Kank1-4* mRNAs and proteins. (A) Total RNA from 8-week-old C57/BL6 mice examined by qRT-PCR. Expression levels were first normalized to *Gapdh* levels and then plotted relative to the expression level of tissue with the lowest expression level, which was spleen in the *Kank1* and *Kank2* analyses, and liver in the *Kank3* and *Kank4* analyses. BM: bone marrow. (B) Characterization of homemade rabbit anti-mouse KANK1-4 antibody specificities using mouse kidney fibroblasts expressing *Kank2*. Stable shRNA-mediated *Kank2* depletion (*shK2*) served as negative control for the KANK2 antibody. *Scr*: scramble shRNA control. Transient transfections of *Kank1*, *Kank3* and *Kank4* cDNAs (+) were used to probe antibody specificities for KANK1, 3 and 4. Arrowheads indicate the specific bands. (C) Western blot of mouse tissue lysates from adult C57/BL6 mice probed with homemade rabbit anti-mouse KANK1, 2, 3 and 4 antibodies.

Fig. 2. KANK1-4 expression in mouse kidney. KANKs are shown in red, Synaptopodin (SYNPO)$^+$ podocytes in blue, PDGFRβ^+ mesangial cells and PECAM$^+$ endothelial cells in green. Nuclei are counterstained with DAPI. (A) KANK1 is expressed in SYNPO$^+$ glomerular podocytes. (B) KANK2 is expressed in SYNPO$^+$ podocytes and PDGFRβ^+ mesangial cells of glomeruli (B1) and in PDGFRβ^+ pericytes surrounding arteries (B2). (C) KANK3 is exclusively present in PECAM$^+$ endothelial cells of glomeruli. (D) KANK4 is expressed in PDGFRβ^+ glomerular mesangial cells. Scale bars: 10 μm.

Fig. 3. Subcellular localization of KANK1 and 2 in mouse podocyte-like cells. KANK1 and 2 are shown in red and Paxillin$^+$ podosomes and focal adhesions in green. Nuclei are counterstained with DAPI. (A, B) Podocytes cultured on LN511 show strong KANK1 (A) and weak KANK2 (B) expression in the outer ring of Paxillin$^+$ podosomes. (C, D) Podocytes cultured on LN111 display KANK1 in the vicinity of Paxillin$^+$ FAs (C) and KANK2 in the belt of FAs and fibrillar adhesions (D). Scale bars: 20 μm.

Fig. 4. KANK1-4 expression in mouse lung. KANKs are shown in red, T1α^+ type I alveolar cells in green or blue, TTF1$^+$ type II alveolar cells in green, PECAM$^+$ endothelial cells in green or blue, and PDGFRβ^+ pericytes in green. Nuclei are counterstained with DAPI. (A) KANK1 is present at the basal side of bronchial epithelial cells and is absent in alveolar cells. (B-D) KANK2 is found in type

I alveolar cells (B; white arrowheads), type II alveolar cells (C; yellow arrowheads) and smooth muscle cells surrounding PECAM$^+$ endothelial blood vessels (D; arrow). The asterisk (D) indicates capillaries decorated by KANK2 expressing pericytes. (E) KANK3 is only expressed in PECAM$^+$ endothelial cells (arrowheads). (F) KANK4 staining is overlapping with PDGFRβ signals, but absent in T1α^+ cells (arrowheads). Scale bars: 20 μm.

Fig. 5. KANK1-3 expression in mouse skin. KANKs are shown in red, PECAM$^+$ endothelial cells and Vimentin$^+$ fibroblasts in green, and Nidogen$^+$ basement membranes in green or blue. Nuclei are counterstained with DAPI. (A) KANK1 is expressed in basal (arrowhead) and suprabasal keratinocytes (arrow). The asterisk indicates KANK1 expression in hair follicles. (B) KANK2 is present in Vimentin$^+$ dermal fibroblasts (B1, arrowhead), pericytes surrounding capillaries (B1, arrow), and Vimentin$^+$ fibroblasts surrounding hair follicles (B2, arrowhead). (C) KANK3 is restricted to PECAM$^+$ endothelial cells. HF, hair follicle. Scale bars: 20 μm.

Fig. 6. KANK1-3 expression in murine brain. KANKs are shown in red and GFAP$^+$ astrocytes, NG2$^+$ pericytes, PECAM$^+$ endothelial cells, Nidogen$^+$ basement membrane and PDGFRβ^+ stromal cells in green. Nuclei are counterstained with DAPI. (A) KANK1 is detected in GFAP$^+$ astrocytes of the medulla oblongata. (B) KANK2 is expressed in pericytes surrounding PECAM$^+$ endothelial cells. (C) KANK3 expression is restricted to PECAM$^+$ endothelial cells. (D) KANK1 is detected at the basal side of ependymal cells of ED14.5 telencephalic choroid plexus. (E) KANK2 is detected in PDGFRβ^+ stromal cells, and (F) KANK3 in PECAM$^+$ endothelial cells of the ED14.5 choroid plexus. Scale bars: 20 μm.

Fig. 7. KANK2 and 3 expression in murine vasculature. KANKs signals are shown in red, αSMA$^+$ smooth muscle cells, PECAM$^+$ endothelial cells, PDGFRβ^+ pericytes, and VEGFR3$^+$ lymphatic endothelial cells in green. Nuclei are counterstained with DAPI. (A-B) KANKs expression in aorta. KANK2 is highly expressed in αSMA$^+$ smooth muscle cells (A) and KANK3 expression is restricted to PECAM$^+$ endothelial cells (B). (C-E) KANKs expression in retina and spleen. (C) showing KANK2 expression in adjacent PDGFRβ^+ pericytes, (D) showing KANK3 staining in PECAM$^+$ endothelial cells of the vascular tube and in tip cells indicated with arrowheads, and (E) showing KANK3 is

463 also expressed in VEGFR3$^+$ lymphatic endothelial cells of the spleen. Asterisks in (B) and (D)
464 indicate non-specific antibody signals. Scale bars: 20 µm.

465 **Fig. 8. KANK1-4 expression in mouse esophagus.** KANKs are shown in red and αSMA$^+$ smooth
466 muscle cells, pan-Cadherin (pan-Cad)$^+$ epithelial cells and PECAM$^+$ endothelial cells in green.
467 Nuclei are counterstained with DAPI. (A) KANK1 expression is restricted to the stratified
468 squamous epithelial cell layers. KANK1 is enriched at the basal side of the basal epithelial cell
469 layer (arrowhead) and diffusely distributed in in the cytoplasm of suprabasal cells. (B) KANK2 is
470 strongly expressed in αSMA$^+$ smooth muscle cells. (C) KANK3 is exclusively expressed in PECAM$^+$
471 endothelial cells (arrowheads), and (D) KANK4 is not expressed in esophagus tissue. The asterisk
472 marks non-specific antibody signals. Scale bars: 20 µm.

473

474

Supplementary Fig. 1. KANK1, 2 and 4 expression in murine kidney. KANKs are shown in red, Synaptopodin (SYNPO)$^+$ podocytes in blue, and PECAM$^+$ endothelial cells and PDGFRβ^+ pericytes in green. Nuclei are counterstained with DAPI. (A) KANK1 is also expressed in epithelial cells of kidney tubules. (B) KANK2 is expressed in SYNPO$^+$ podocytes of glomeruli but absent in PECAM$^+$ endothelial cells. (C) KANK4 is expressed in PDGFRβ^+ pericytes of blood vessels. Scale bars: 10 μm.

Supplementary Fig. 2. KANK1-4 antibodies on kidney sections from KANK1-, 2-, 3-, 4-null mice. KANK1-4 are shown in red, and Synaptopodin (SYNPO)$^+$ podocytes in green. Nuclei are counterstained with DAPI. No obvious signals are detected in respective KANK-null tissues, confirming antibody specificity. Scale bars: 20 μm.

Supplementary Fig. 3. KANK2 and 3 expression in murine retina. KANKs signals are shown in red, PECAM$^+$ endothelial cells and PDGFRβ^+ pericytes in green. (A) No KANK2 expression in PECAM$^+$ endothelial cells (arrowheads). (B) No KANK3 expression in PDGFRβ^+ pericytes (arrows). Scale bars: 20 μm.

Supplementary Tables

Table S1: Primers used for quantitative RT-PCR

Gene	Primer	Sequence
Gapdh	Forward	5’-AAGGTCATCCCAGAGCTGAACG-3’
	Reverse	5’-CCTCAGATGCCTGCTTCACCA-3'
Kank1	Forward	5’-GAACTCTGACTTCCAGAAAGCCA-3’
	Reverse	5’-TACATTTAACAGTCCTCCTGACCG-3’
Kank2	Forward	5’-GCATGAACATCAAGTGCTCGTT-3’
	Reverse	5’-TTTGATGCGTGGCTTGTGG-3’
Kank3	Forward	5’-ACCACACAGACAGAGCTGCCAGT-3’
	Reverse	5’-CTGACTGGATTGTGCACCTGGA-3’
Kank4	Forward	5’-GACTTGCATCCCAGCTGTGAGG-3’
	Reverse	5’-TGGCACGCGTTAAGAAATTCCT-3’

Table S2: Mouse peptide sequence used to generate rabbit antisera

Antibody	Sequence
KANK1	CPRLGRKTSPGPTHRG
KANK2	CKRKEDPADPEVNQRN
KANK3	GTPGPHNDKDAGDC
KANK4	QGDEEKEPPKSYPYSC

Table S3: Antibody dilutions

1st Antibody	Source	Concentration
KANK1	Homemade	1:1000 (WB), 1:2000 (IF)
KANK1	Sigma, HPA056090	1:1000 (WB, IF)
KANK2	Homemade	1:1000 (WB), 1:4000 (IF)

KANK2	Sigma, HPA015643	1:2000 (WB, IF)
KANK3	Homemade	1:1000 (WB), 1:6000 (IF)
KANK3	Sigma, HPA051153	1:1000 (WB, IF)
KANK4	Homemade	1:1000 (WB), 1:4000 (IF)
KANK4	Sigma, HPA014030	1:1000 (WB, IF)
Tubulin	Milipore MAB1864	1:1000 (WB)
PECAM-1	PharMingen 553370	1:600 (IF)
TTF1*	NSJ Bioreagents V7084	1:200 (IF)
T1α	R&D systems AF3244	1:400 (IF)
Synaptopodin	Santa Cruz, sc-21537	1:200 (IF)
PDGFRβ	Abcam, ab91066	1:400 (IF)
Nidogen	Millipore, MAB1946-I	1:2000 (IF)
αSMA	Sigma, A2547	1:400 (IF)
Paxillin	Transduction Laboratories, 610051	1:400 (IF)
GFAP	Abcam, ab4674	1:5000 (IF)
NG2	Millipore, MAB5384	1:200 (IF)
Pan-cadherin	Santa Cruz, sc-1499	1:600 (IF)
Vimentin	Abcam, ab24525	1:2000 (IF)
VEGFR3/FH-4	R+D Systems, AF743	1:200 (IF)
2nd Antibody	**Source**	**Concentration**
Donkey α-rabbit^{Cy3}	Jackson Lab, 711-165-152	1:800 (IF)
Donkey α-rat^{Alexa488}	Life technologies, A21208	1:800 (IF)
Goat α-rat^{Alexa647}	Invitrogen, A21247	1:500 (IF)
Donkey α-mouse^{Alexa488}	Invitrogen, A21202	1:800 (IF)
Donkey α-mouse^{Alexa647}	Invitrogen, A31571	1:500
Donkey α-goat^{Alexa647}	Invitrogen A21447	1:500 (IF)

*Antigen retrieval is required (Citric buffer, pH 6.0, boil for 15 min)

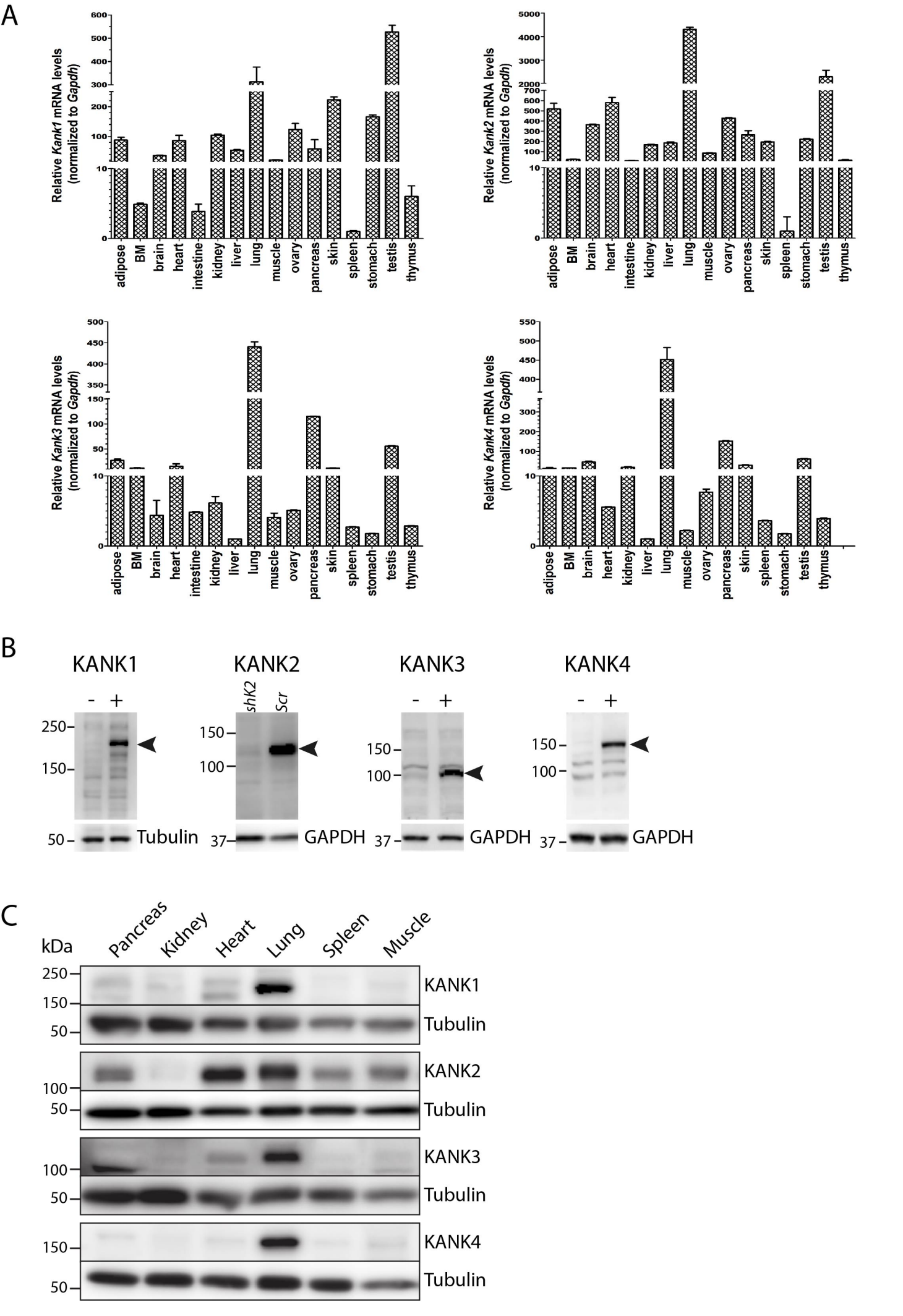

Guo et al., Figure 1A-C

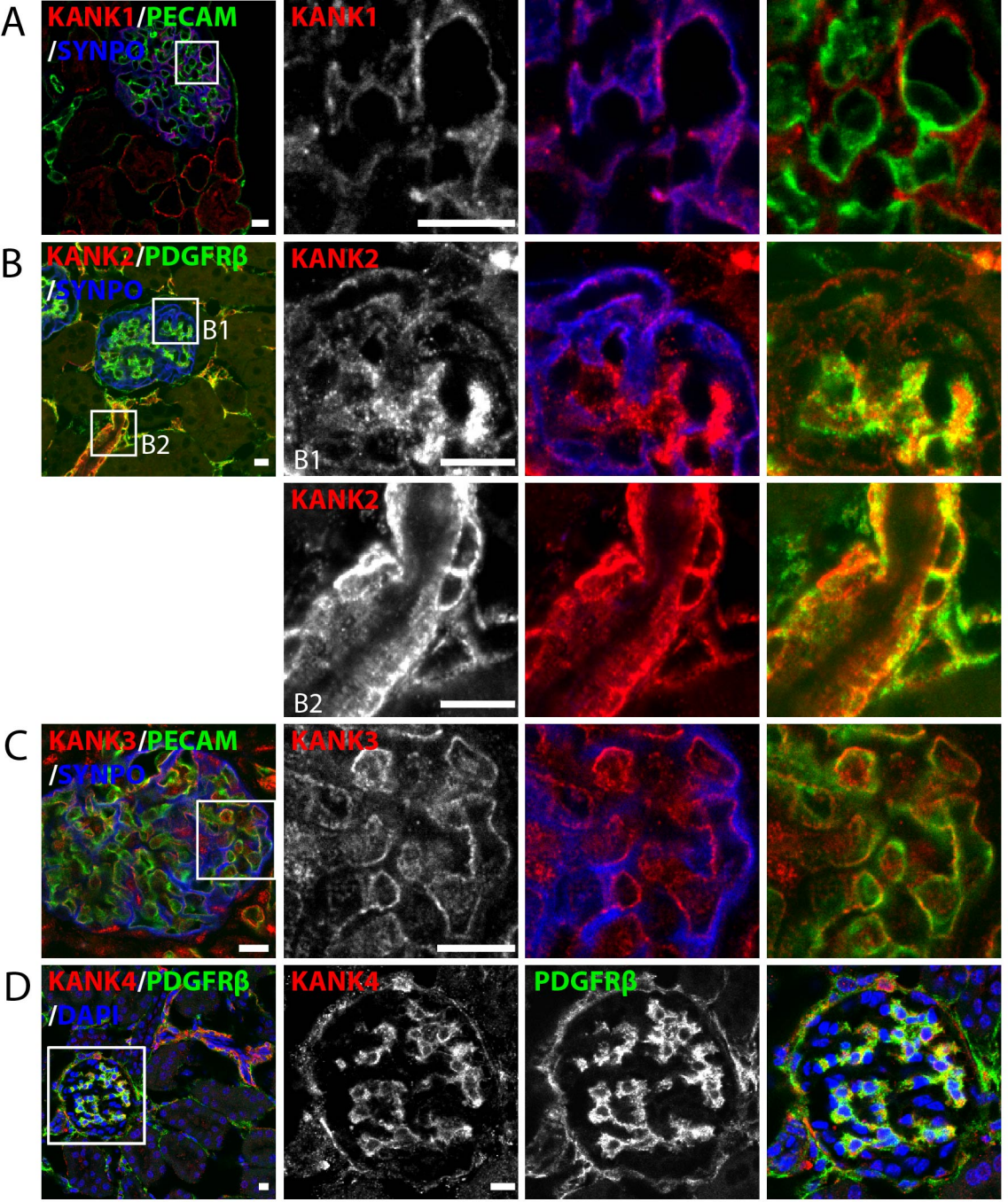

Guo et al., Figure 2A-D

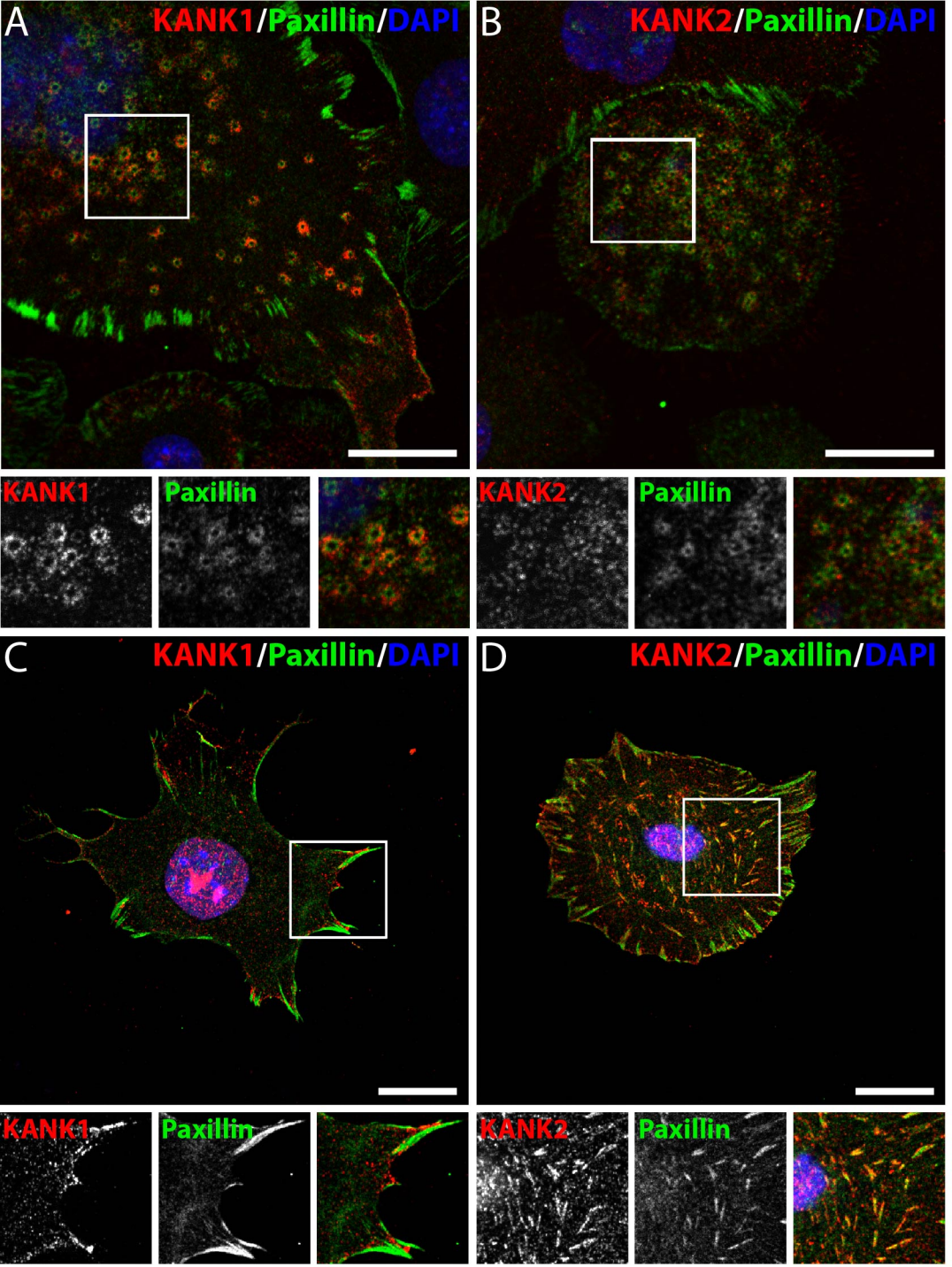

Guo et al., Figure 3A-D

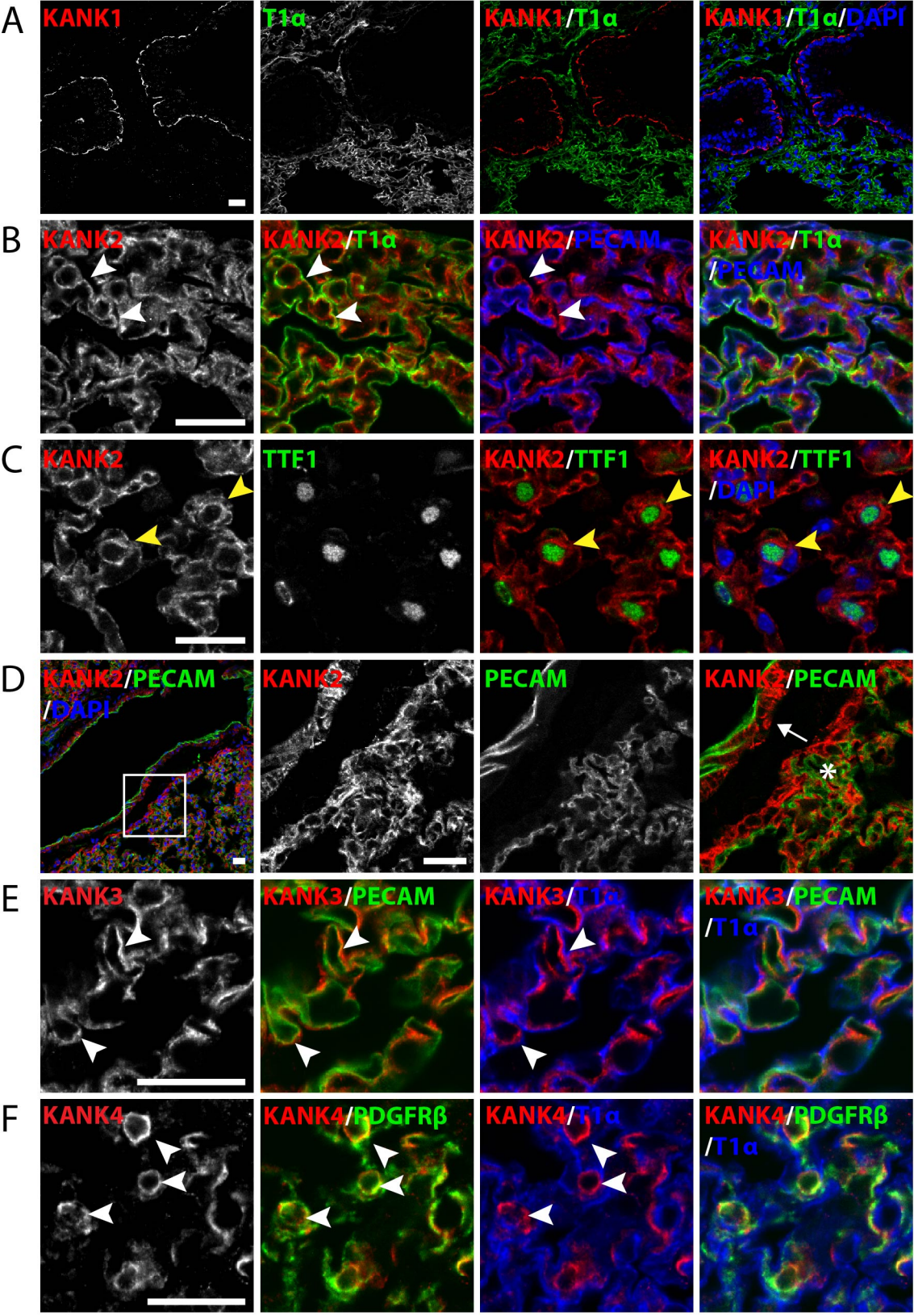

Guo et al., Figure 4A-F

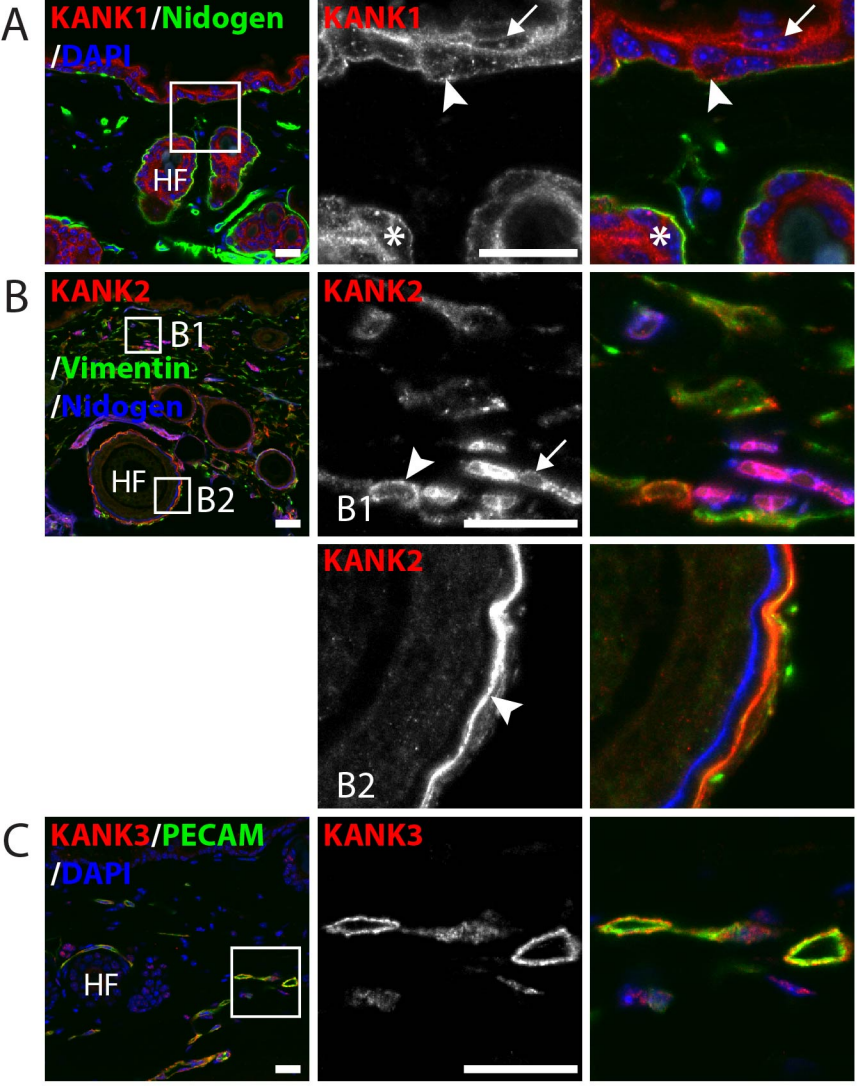

Guo et al., Figure 5A-C

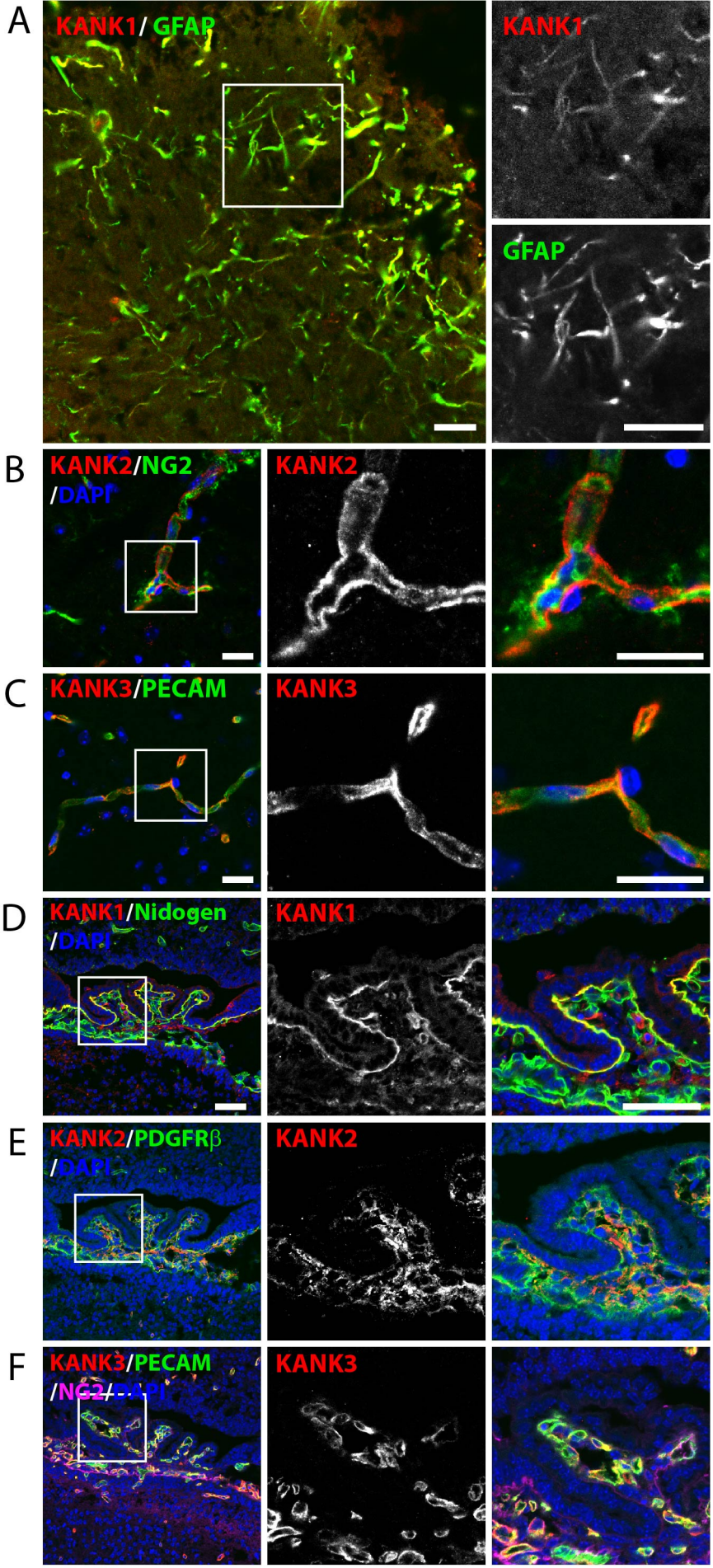

Guo et al., Figure 6A-F

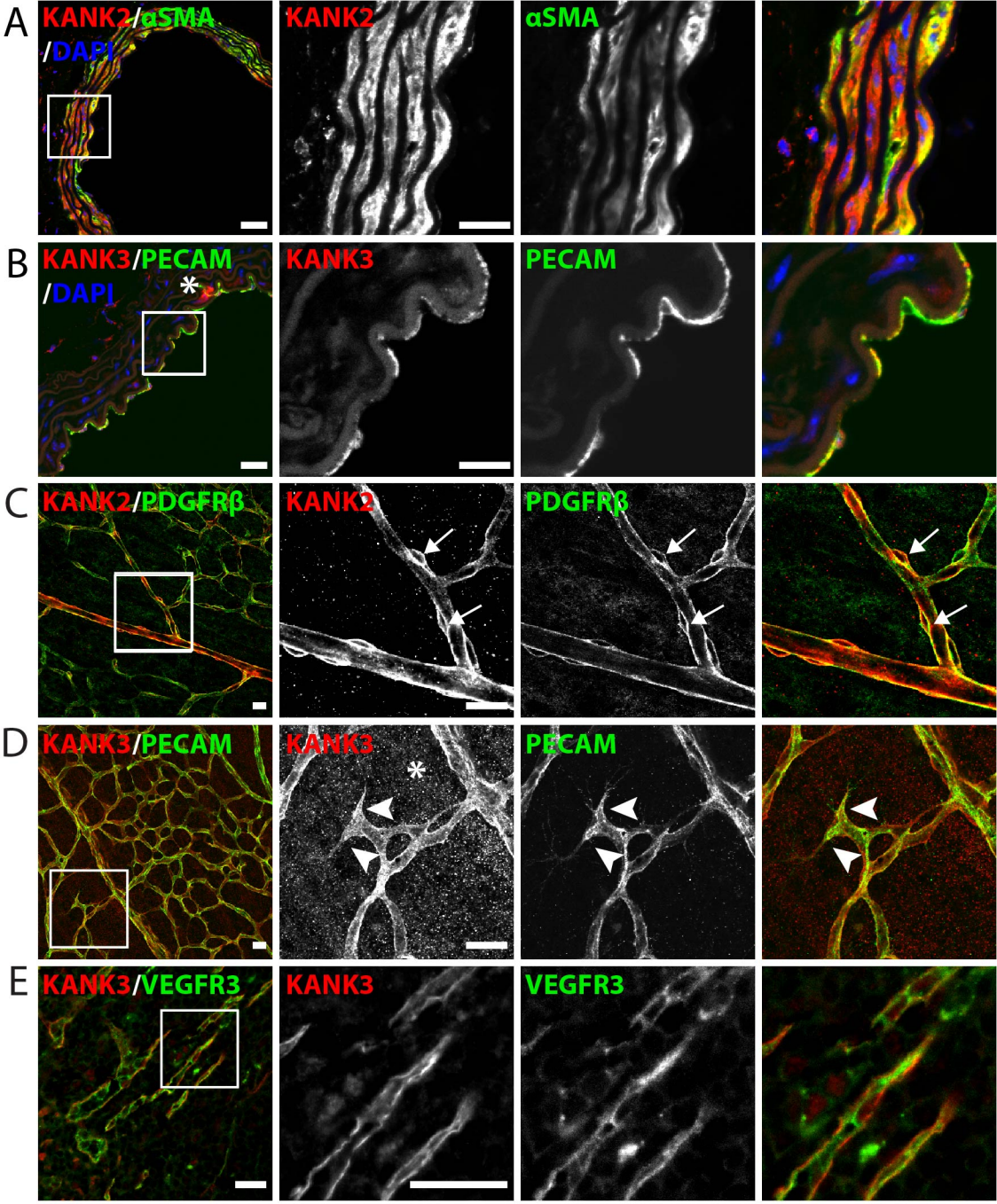

Guo et al., Figure 7A-E

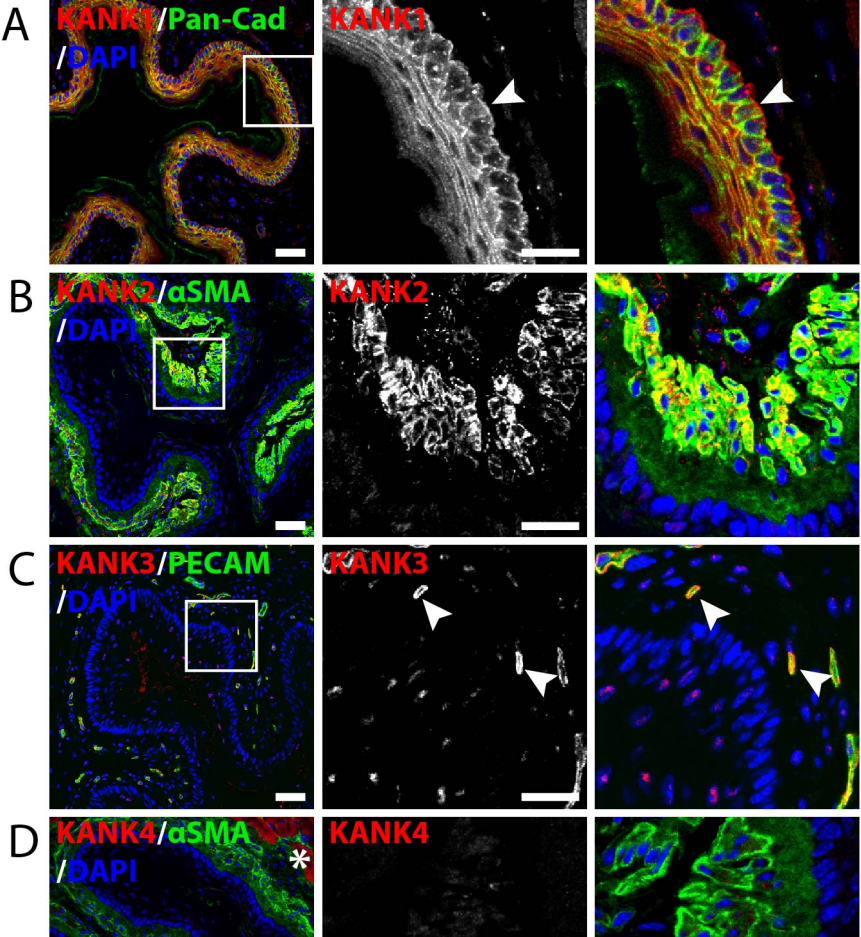

Guo et al., Figure 8A-D

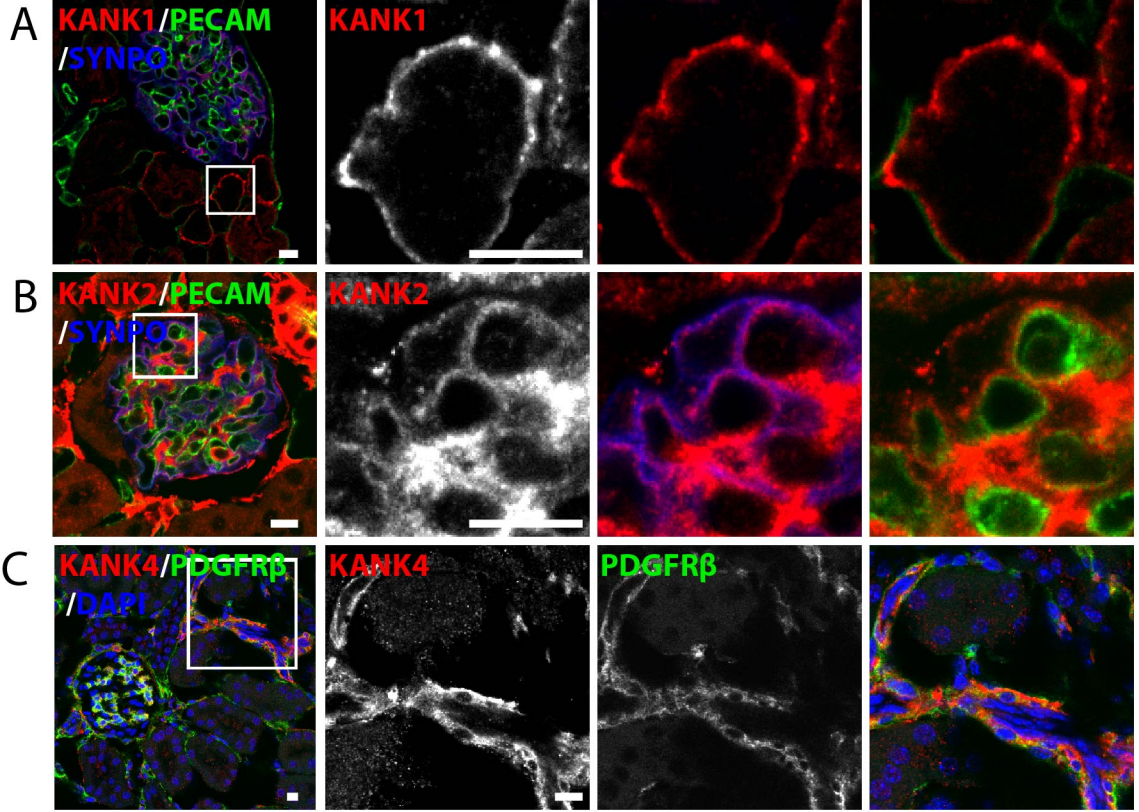

Guo et al., Supp Figure 1A-C

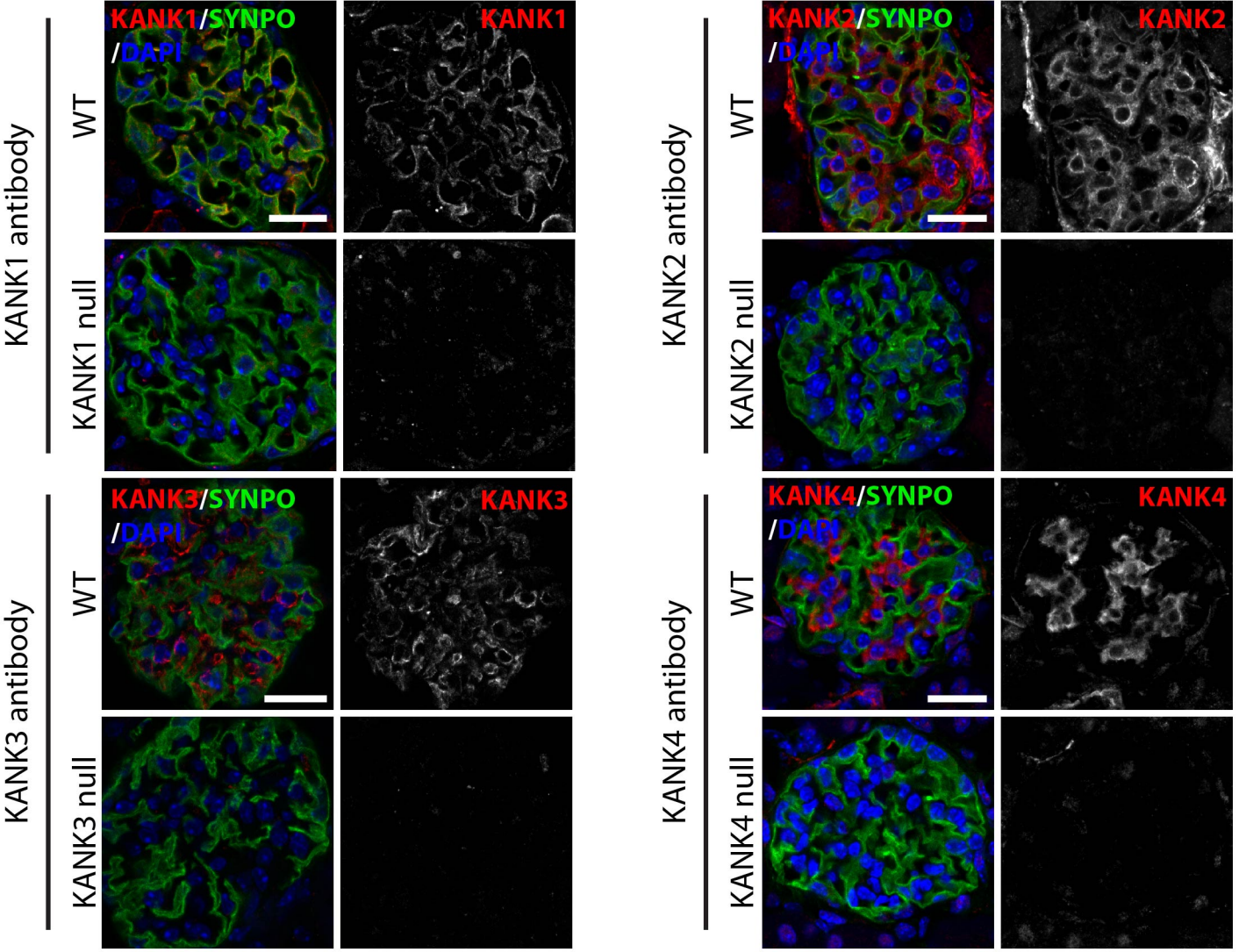

Guo et al., Supp Figure 2

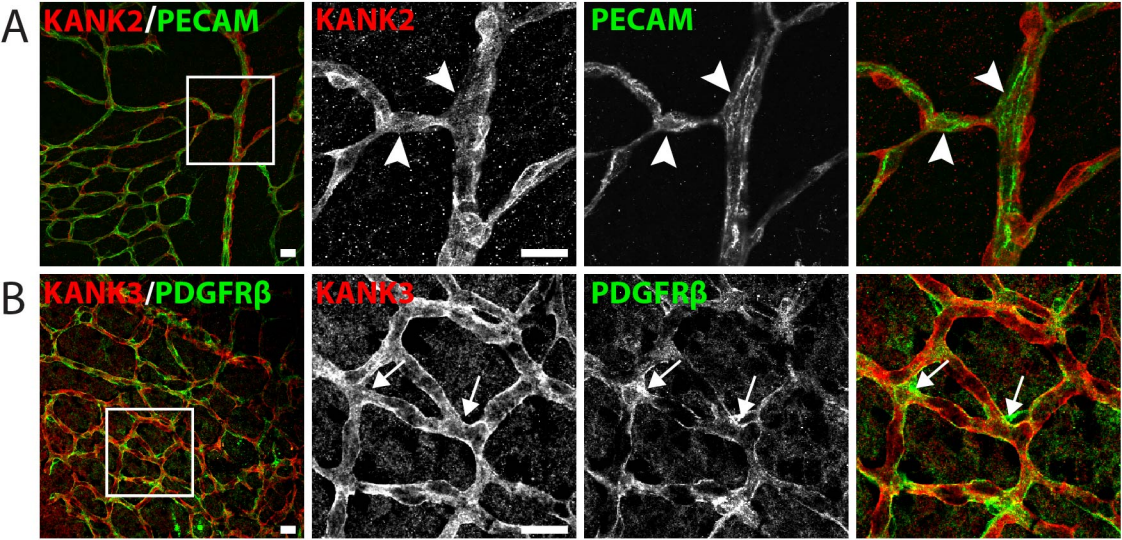

Guo et al., Supp Figure 3A-B